Electronic Supplementary Material (ESI) for Inorganic Chemistry Frontiers.

Supplementary Material

PEO/$Li_{1.25}Al_{0.25}Zr_{1.75}(PO_4)_3$ Composite Solid Electrolytes for High-Rate and Ultra-Stable All-Solid-State Lithium Metal Batteries with Impregnated Cathode Modification

Yongquan Zhang,[a] Hongchang Gao,[a] Jingshun Wang,[a] Qingguo Chi,*[a] Tiandong Zhang,[a] Changhai Zhang,[a] Yu Feng,[a] Yue Zhang,[a] Dianxue Cao[b] and Kai Zhu*[b]

[a] Key Laboratory of Engineering Dielectrics and Its Application (Ministry of Education), School of Electrical and Electronic Engineering, Harbin University of Science and Technology, Harbin 150080, P. R. China

[b] Key Laboratory of Superlight Materials and Surface Technology (Ministry of Education), College of Materials Science and Chemical Engineering, Harbin Engineering University, Harbin 150001, P. R. China

***Corresponding author**

E-mail: qgchi@hotmail.com (Q. Chi).

E-mail: kzhu@hrbeu.edu.cn (K. Zhu).

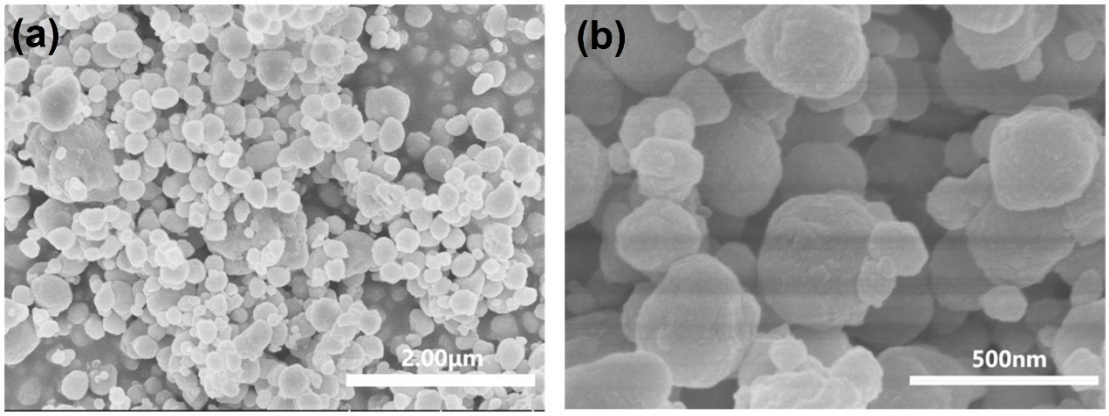

Fig. S1 (a) and (b) SEM image of LAZP ceramic powder.

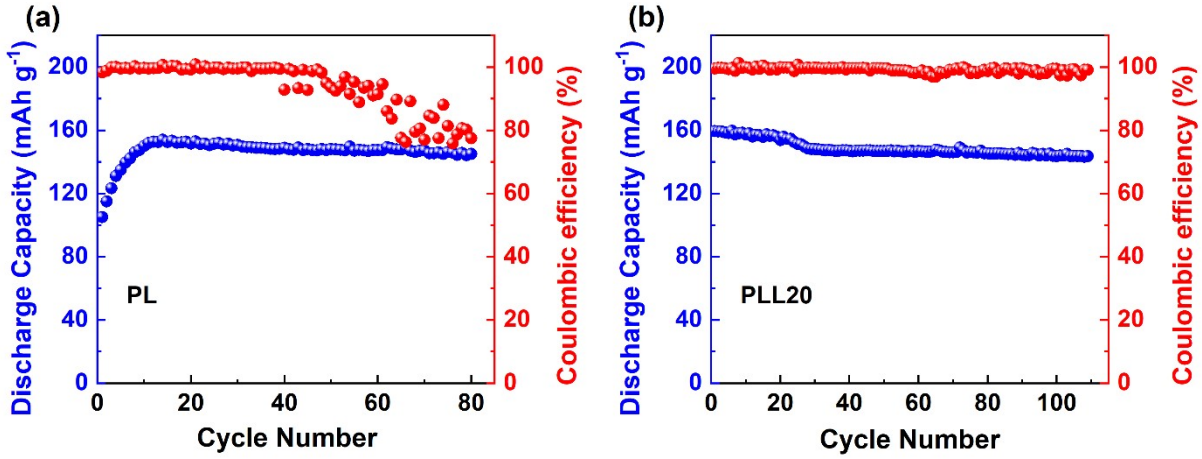

Fig. S2 Cyclic performance of (a) LFP/PL/Li battery and (b) LFP/PLL20/Li battery at 60°C and 0.2C.

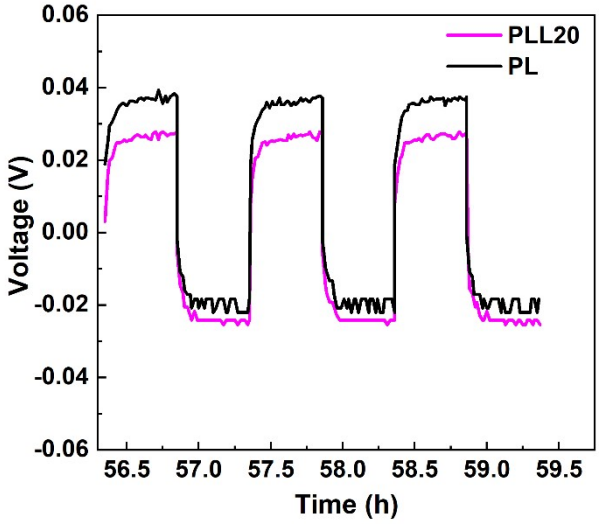

Fig. S3 Galvanostatic cycling performance of Li/PL/Li and Li/PLL20/Li symmetrical cells with 0.1 mA cm^{-2} current densities at 60°C.

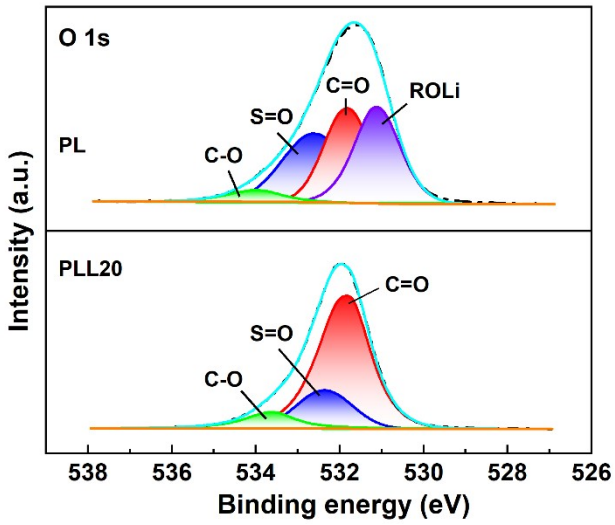

Fig. S4 XPS spectra of O1s for cycled Li anodes.

In the O 1s spectrum of Li metal in Li|PL|Li cell, the peaks located at 531.11, 531.8, 532.6, and 533.94 eV are assigned to ROLi, C=O, S=O, and C-O, respectively. From the O 1s spectrum of Li metal in Li|PLL20|Li cell, the binding energy at 531.8, 532.36, and 533.57 eV are assigned to C=O, S=O, and C-O, respectively.[1-3] The C=O and C-O could be attributed to the decomposition of PEO-LiTFSI at the interface. In addition, S=O peak should come from LiTFSI.[4] It is worth noting that the lithium alkoxides (ROLi)[5] peak does not exist in PLL20, which means that LAZP reduces the generation of ROLi, making the relationship between PLL20 and Li metal interface layer more stable.

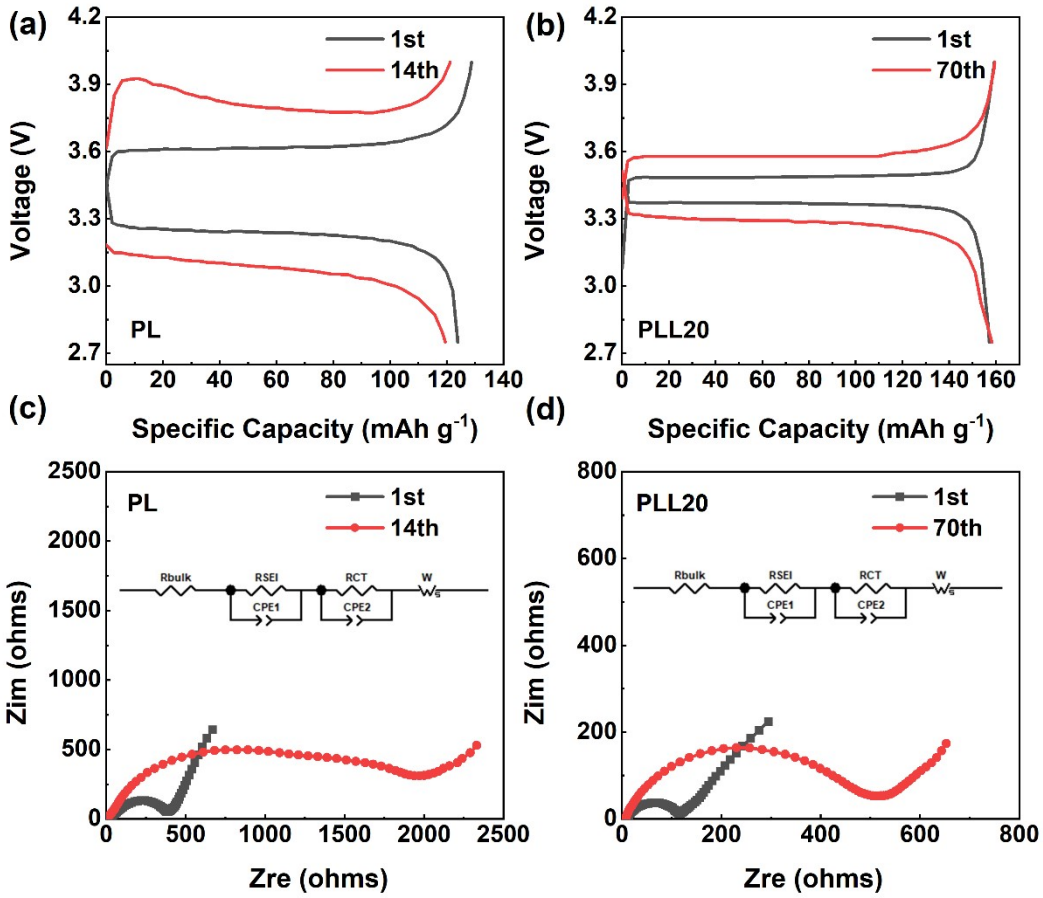

Fig. S5 (a) The first and fourteenth charge-discharge curves of Li/PL/LFP batteries at 2C. (b) The first and seventieth charge-discharge curves of Li/PLL20/LFP battery at 2C. (c) The impedance spectra of the first and fourteenth cycles of the Li/PL/LFP battery. (d) The impedance spectra of the first and seventieth cycles of the Li/PLL20/LFP battery.

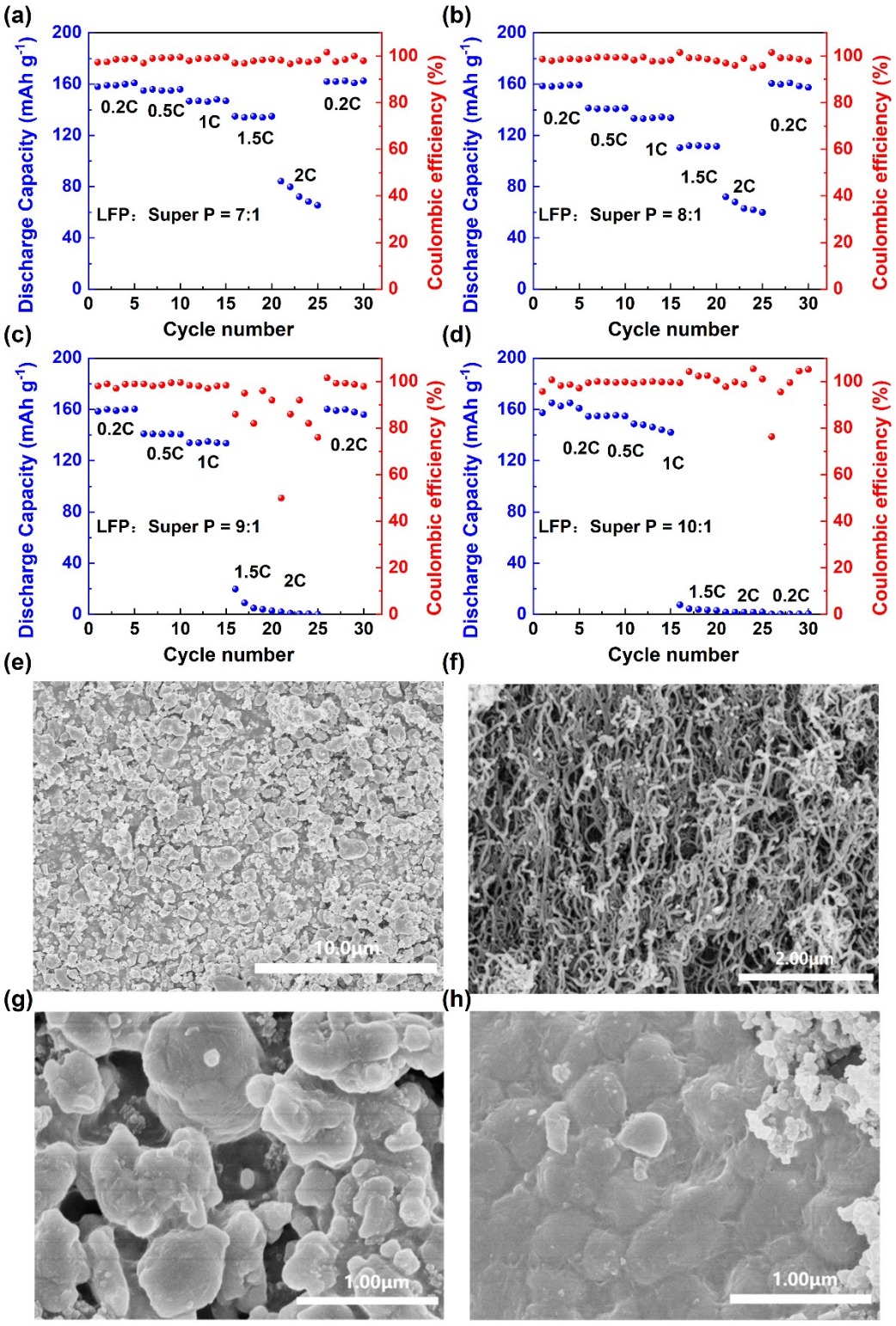

Fig. S6 Rate performances of Li//LFP cell at 60℃, LFP: Super P=7:1 (a), LFP: Super P =8:1 (b), LFP: Super P =9:1 (c), and LFP: Super P =10:1 (d). SEM of LFP powder (e), MWCNT (f), Unmodified LFP cathode (g), and M-LFP (h).

In order to investigate the effect of composition and ratio of LFP cathode material on solid electrolyte. The electrochemical properties of LFP cathode material were studied by modifying it. LFP powder was selected as the positive active material; Super P as the electronic conductive agent; PVDF as the binder; PEO and LiTFSI are used to increase ionic conductivity in composite positive electrodes; MWCNT are used to construct long-range conductive channels. The mass of MWCNT and PEO-LITFSI is fixed, and the mass ratio of LFP to Super P is different. The amount of Super P determines the overall electrochemical performance of the composite positive electrode. If the content of Super P is small, the $LiFePO_4$ cannot be fully coated, resulting in low electrical conductivity of the composite positive electrode, resulting in the reduction of high-rate specific capacity. All-solid-state batteries assembled with PL solid electrolyte were tested at 60℃. As shown in **Fig. S6a-d**, with the increasing of Super P content, the specific capacity attenuation of all-solid-state battery decreases gradually at variable magnification. When the mass ratio of LFP to Super P is 10:1, the specific capacity of the all-solid-state battery decreases obviously with the increase of current density at high magnification, which seriously affects the performance of the all-solid-state battery at high magnification. This stems from the fact that less Super P leads to poor electronic conductivity in the composite positive electrode. Finally, the mass ratio of LFP to Super P was determined to be a more appropriate ratio of 7:1. In this study, the size of LFP powder was between 1-4 μm (**Fig. S6e**). As a common electronic conductor, Super P has the advantages of small particle size, strong liquid absorption capacity, large specific surface area, etc., but its disadvantage is that it cannot form a long-term continuous conductive path, and during the long cycle of the battery, the point contact between it and the lithium iron phosphate particles will deteriorate, resulting in the decline of the specific capacity of the battery and the service life of the battery.[6, 7] In order to solve this problem, an appropriate amount of MWCNT is usually added to the composite positive electrode, which is used as a 1D filler, as shown in **Fig. S6f**. The size is between 3-8 μm, which can connect more LFP powder and Super P particles on a spatial scale, thus forming a long-range electronic conductive path.[8, 9] While improving the electronic conductivity in the composite positive electrode, it

can also better connect the nanoparticles in the composite positive electrode, thereby reducing the specific capacity loss of the battery during the long cycle process and extending the service life of the battery. SEM shows that all LFP is uniformly coated with a thin-film structure around it, which is shown as PVDF polymer in **Fig. S6g** and a mixture of PVDF and PEO electrolyte in **Fig. S6h**. The composite positive electrode containing PEO electrolyte is relatively dense, and the nanoparticles are uniformly coated by the polymer without voids, while the composite positive electrode without PEO electrolyte has a certain amount of voids on its surface. This phenomenon is conducive to increasing the contact area between the composite electrolyte and the composite positive electrode, and increasing the ion transport area, which is conducive to ion transport. In addition, the addition of PEO[10] and LiTFSI[11] will enhance the ionic conductivity of the composite positive electrode, and PEO will fully cover the nanoparticles. Due to its high viscosity and good interface wettability, on the one hand, it can inhibit the volume expansion of the electrode during the cycle. On the other hand, the high interface impedance caused by the solid-solid contact between the composite electrolyte and the composite positive electrode can be reduced.

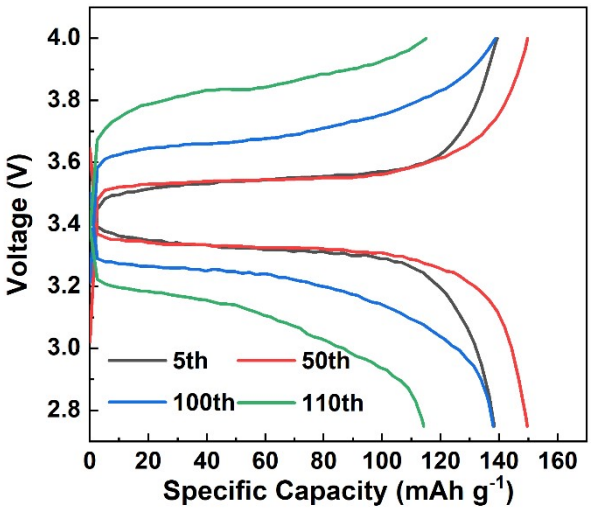

Fig. S7 Charge-discharge profiles of the Li/PLL20/LFP batteries at 60℃ and 1C.

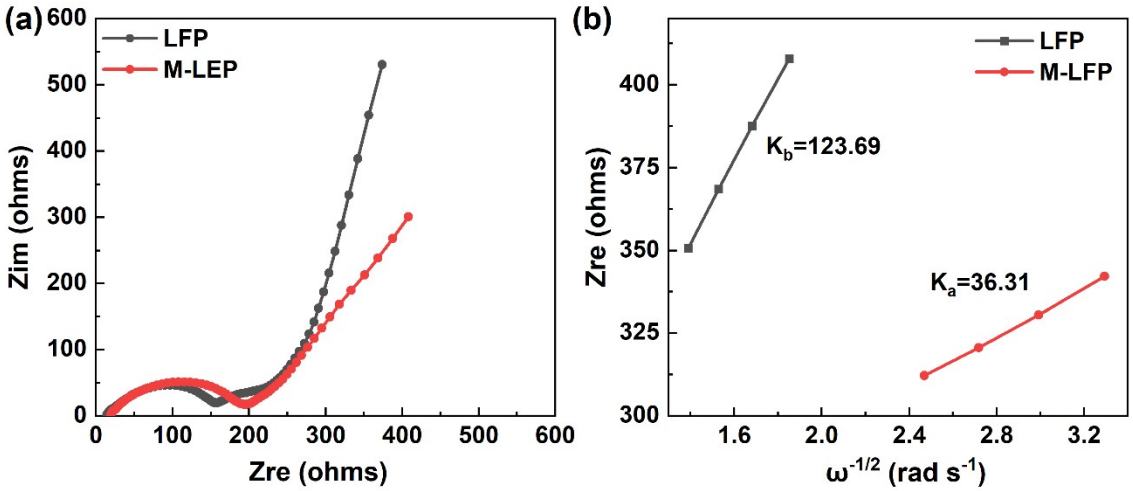

Fig. S8 (a) AC impedance spectra of the Li/PLL20/LFP cell and the Li/PLL20/M-LFP batteries at 60℃. (b) Fitting graph of the relationship between Z_{re} and $\omega^{-1/2}$.

Table S1. Study on the PEO-based CSEs for LFP batteries.

Research Team	CSEs	Ionic conductivity (10^{-4} S cm^{-1})	Discharge rate	Cycle number	Discharge specific Capacity (mAh g^{-1})[a]	Capacity retention rate (%)
Huang[12]	PEO/CMC-Li@PI	3.15	0.5C	150	93	82
Zheng[13]	PEO/PCN/LiTFSI	3.47	0.5C	1000	149	57
Zeng[14]	PEO@AF	6.57	1C	100	115.6	94.3
Wu[15]	PEO-n-UIO	1.3	0.5	100	144	95.4
Liang[16]	PEO−MA@LAGP	4.2	1C	100	147	71
Wang[17]	Z-C-PAN-PEO	4.39	0.2C	600	161	68
Our work	PPL20	8.6453	1 C	200	144	93.5

[a] Discharge specific capacity refers to the value of the last circle of the cycle.

References

1 T. Y. Wang, X. L. Zhang, N. Yuan and C. W. Sun, Molecular Design of a Metal-Organic Framework Material Rich in Fluorine as an Interface Layer for High-Performance Solid-State Li Metal Batteries, *Chem. Eng. J.*, 2023, **451**, 138819.

2 Q. Yi, W. Q. Zhang, T. Y. Wang, J. X. Han and C. W. Sun, A High-performance Lithium Metal Battery with a Multilayer Hybrid Electrolyte, *Energy Environ. Sci.*, 2023, **6**, e12289.

3 C. Xu, B. Sun, T. Gustafsson, K. Edström, D. Brandell and M. Hahlin, Interface Layer Formation in Solid Polymer Electrolyte Lithium Batteries: an XPS Study, *J. Mater. Chem. A*, 2014, **2**, 7256-7264.

4 X. Ye, J. N. Liang, J. T. Hu, D. Z. Wu, Y. L. Li, X. P. Ouyang, Q. L. Zhang, X. Z. Ren and J. H. Liu, An Ultra-Thin Polymer Electrolyte for 4.5 V High Voltage $LiCoO_2$ Quasi-Solid-State Battery, *Chem. Eng. J.*, 2023, **455**, 140846.

5 E. E. Ushakova, A. Frolov, A. A. Reveguk, D. Y. Usachov, D. M. Itkis and L. V. Yashina, Solid Electrolyte Interface Formation between Lithium and PEO-Based Electrolyte, *Appl. Surf. Sci*., 2022, **589**, 153014.

6 Q. Wang, F. Y. Su, Z. Y. Tang, G. W. Ling and Q. H. Yang, Synergetic effect of conductive additives on the performance of high power lithium ion batteries, *New Carbon Mater.*, 2012, **27**, 427-432.

7 K. B. Dermencia, S. Turana, M. Behm and G. Lindbergh, Effect of Cathode Slurry Composition on the Electrochemical Properties of Li-ion Batteries, *ECS Trans.*, 2015, **66**, 285-293.

8 C. Niu, E. K. Sichel, R. Hoch, D. Moy and H. Tennent, High power electrochemical capacitors based on carbon nanotube electrodes, *Appl. Phys. Lett.*, 1997, **70**, 1480-1482.

9 Q. Zhang, G. Peng, J. P. Mwizerwa, H. L. Wan, L. T. Cai, X. X. Xu and X. Y. Yao, Nickel sulfide anchored carbon nanotubes for all solid-state lithium batteries with enhanced rate capability and cycling stability, *J. Mater. Chem. A*, 2018, **6**, 12098-12105.

10 C. H. Tsao, C. H. Hsu and P. L. Kuo, Ionic Conducting and Surface Active Binder of Poly (ethylene oxide)-block-poly(acrylonitrile) for High Power Lithium-ion Battery, *Electrochim. Acta*, 2016, **196**, 41-47.

11 D. Mohanty, P. H. Huang and I. M. Hung, Preparation and Characterization of a $LiFePO_4$-Lithium Salt Composite Cathode for All-Solid-State Li-Metal Batteries, *Batteries*, 2023, **9**, 236.

12 X. W. Huang, S. Y. Liao, Y. D. Liu, Q. S. Rao, X. K. Peng and Y. G. Min, Design, fabrication and application of PEO/CMC-Li @PI hybrid polymer electrolyte membrane in all-solid-state lithium

battery, *Electrochim. Acta*, 2021, **389**, 138747.

13 J. H. Wei, X. W. Zheng, W. T. Lin, Y. Si, K. M. Ji, C. Y. Wang and M. M. Chen, Retarding Li dendrites growth via introducing porous g-C_3N_4 into polymer electrolytes for solid-state lithium metal batteries, *J. Alloys Compd.*, 2022, **909**, 164825.

14 F. Y. Zeng, Y. Y. Sun, B. Hui, Y. Z. Xia, Y. H. Zou, X. L. Zhang and D. J. Yang, Three-Dimensional Porous Alginate Fiber Membrane Reinforced PEO-Based Solid Polymer Electrolyte for Safe and High-Performance Lithium Ion Batteries, *ACS Appl. Mater. Interfaces*, 2020, **12**, 43805-43812.

15 J. F. Wu and X. Guo, MOF-derived nanoporous multifunctional fillers enhancing the performances of polymer electrolytes for solid-state lithium batteries, *J. Mater. Chem. A*, 2019, **7**, 2653-2659.

16 Y. H. Liang, N. Chen, F. Li and R. J. Chen, Melamine-Regulated Ceramic/Polymer Electrolyte Interface Promotes High Stability in Lithium-Metal Battery, *ACS Appl. Mater. Interfaces*, 2022, **14**, 47822-47830.

17 L. Y. Wang, L. L. Dong, Z. T. Wang, S. G. Enbo, J. Li, L. P. Li, S. B. Gao and N. P. Deng, Engineering 3D Interpenetrated ZIF-8 Network in Poly(ethylene oxide) Composite Electrolyte for Fast Lithium-Ion Conduction and Effective Lithium-Dendrite Inhibition, *ACS Sustainable Chem. Eng.*, 2023, **11**, 9337-9348.